Hydrol. Earth Syst. Sci. Discuss., 10, 5643–5686, 2013
www.hydrol-earth-syst-sci-discuss.net/10/5643/2013/
doi:10.5194/hessd-10-5643-2013

Hydrology and Earth System Sciences
Open Access
Discussions

Riparian forest and permanent groundwater: a key coupling for balancing the hillslope water budget in Sudanian West Africa

A. Richard[1], S. Galle[2], M. Descloitres[2], J. M. Cohard[1], J. P. Vandervaere[1], L. Séguis[3], and C. Peugeot[3]

[1]UJF-Grenoble 1, LTHE, UMR5564, CNRS – UJF-Grenoble 1/G-INP/IRD, 38041 Grenoble, France
[2]IRD, LTHE, UMR5564, CNRS – UJF-Grenoble 1/G-INP/IRD, 38041 Grenoble, France
[3]IRD, HSM, UMR5569, CNRS – UM1/UM2, 34095 Montpellier, France

Received: 23 March 2013 – Accepted: 19 April 2013 – Published: 2 May 2013

Correspondence to: A. Richard (alois.richard@ujf-grenoble.fr)

Published by Copernicus Publications on behalf of the European Geosciences Union.

Abstract

Forests are thought to play an important role in the regional dynamics of the West African monsoon, through their capacity to extract water from permanent aquifers located deep in the soil and pump it into the atmosphere even during the dry season. This is especially true for riparian forests located at the bottom of the hillslopes. This coupling between the riparian forests and the permanent aquifers is investigated, looking for quantifying its contribution to the catchment water balance. To this end, use is made of the observations available from a comprehensively instrumented hillslope through the framework of the AMMA-CATCH (African Monsoon Multidisciplinary Analysis – Coupling the Tropical Atmosphere and the Hydrological Cycle) observing system. Attention is paid to measurements of actual evapotranspiration, soil moisture and deep groundwater level. A vertical 2-D approach is followed using the physically-based Hydrus 2-D model in order to simulate the hillslope hydrodynamics, the model being calibrated and evaluated through a multi-criteria approach.

The model correctly simulates the hydrodynamics of the hillslope as far as soil moisture dynamics, deep groundwater fluctuation and actual evapotranspiration dynamics are concerned. In particular, the model is able to reproduce the observed hydraulic disconnection between the deep permanent groundwater table and the river. A virtual experiment shows that the riparian forest depletes the deep groundwater table level through transpiration occurring throughout the year so that the permanent aquifer and the river are not connected. Moreover the riparian forest and the deep groundwater table form a coupled transpiration system: the riparian forest transpiration is due to the water redistribution at the hillslope scale feeding the deep groundwater through lateral saturated flow. The annual cycle of the transpiration origin is also quantified. The riparian forest which covers only 5 % of the hillslope generates 37 % of the annual transpiration, this proportion reaching 57 % during the dry season. In a region of intense anthropogenic pressure, forest clearing and its replacement by cropping could

HESSD
10, 5643–5686, 2013

impact significantly the water balance at catchment scale with a possible feedback on the regional monsoon dynamics.

1 Introduction

The West African climate is characterised by strong interactions between the atmosphere, the ocean and the land surfaces. During the wet season, the ocean brings moisture to the continent through a typical atmospheric monsoon circulation driven by meridional energy and moisture gradients. Moisture availability in the regions located around 10° N is found to be pivotal for the West African Monsoon (WAM) dynamics (Lebel and Ali, 2009). Vegetation at this latitude is abundant and the trees of the riparian forests are evergreen, potentially providing humidity to the atmosphere even during the dry season. It is suspected that this reservoir of water plays a major role for the WAM onset into the Sahel (Fontaine et al., 1999; Philippon and Fontaine, 2002). While it physically makes sense that continentally stored water plays a role in the monsoon dynamics, it must be acknowledged that very little is known on the functioning of these riparian forests which, beyond climatological considerations, largely control the local water cycle. This paper precisely aims to provide a better understanding the local water cycle in the hydrological system formed by hillslopes, riparian forests and underlying groundwater in regions of Sudanian climate, where riparian forests are a key element of the landscape. As such it intends to contribute to a better closing of the water balance both at local and at larger scales, which can benefit to hydrologists and climatologists.

The AMMA-CATCH observing system (Lebel et al., 2009) provides an unprecedented set of data to explore this issue. One AMMA-CATCH site is the Ouémé catchment located in northern Benin (Fig. 1). An ensemble of nested catchments is equipped with rainfall, streamflow, groundwater and evapotranspiration measurements, allowing for the study of the hydrological processes and associated water budgets from the mesoscale (Peugeot et al., 2011) down to the hillslope scale (Guyot et al., 2009; Séguis et al., 2011a). Prior to the establishment of the AMMA-CATCH monitoring, studies

HESSD
10, 5643–5686, 2013

conducted in Ivory Coast have shown that, in regions of comparable climate and land cover to the one prevailing in northern Benin, a significant proportion of the streamflow of headwater catchments is generated by subsurface fluxes (Lafforgue, 1982; Chevallier and Planchon, 1993; Masiyandima et al., 2003). Similar behaviour was observed over the smallest of the AMMA instrumented catchments in Benin, namely the Ara catchment (12 km^2) and the Aguima catchment (16.5 km^2) (Giertz and Diekkrüger, 2003). In such a context, the contribution of deep permanent groundwater to surface streamflow has long been disputed. A series of hydrodynamic, geochemical and subsurface geophysical investigations (Kamagaté et al., 2007; Séguis et al., 2011b) have shown this contribution to be negligible at the intermediate scale of the Donga catchment (586 km^2), leaving open the possibility that the permanent aquifers participate to the water cycle only at regional scale.

Applying the above knowledge in models produced inconsistent results. For one, by taking into account hillslope processes (overland flow and interflow) in an enhanced 1-D Soil-Vegetation-Atmosphere Transfer (SVAT) model, Giertz et al. (2006) correctly simulated the streamflow of the 16.5 km^2 Aguima catchment. At a larger scale, Le Lay et al. (2008) used a TopModel approach (Beven and Kirkby, 1979; Beven, 1997) to simulate the discharge at the outlet of the Donga catchment. The 4 parameters of the model were calibrated in order to reproduce as best as possible the Donga discharge, which required the introduction of a deep infiltration term, not originally present in the model. The relevance of this term is highly questionable since the observations available in the deep aquifers show no time variability that should result from such deep percolation. It is thus likely that this component that has been added to the water budget has the hidden role of compensating either an underestimated evapotranspiration – a term not well paramatrized in the model – or underestimated subsurface lateral exchanges. In other words equifinality and calibration procedures (see e.g. Beven, 2001), associated with the lack of observed diagnostic variables make it uncertain that the Donga discharge is correctly simulated because processes are well represented. Along these lines, a recent review by Peugeot et al. (2011) shows that the hydrological and

HESSD
10, 5643–5686, 2013

SVAT models used to represent the mesoscale water cycle over the Ouémé catchment agree on streamflow simulation but that at the same time they differ significantly in evapotranspiration and water storage terms. Consequently, and following the recommendations of Tromp-van Meerveld and Weiler (2008), Peugeot et al. (2012) further point out that evaluating the relevance of models require data documenting internal state and diagnostic variables of these models so that the output variable (the discharge) is not used as the only benchmark for judging the quality of a model.

Since evapotranspiration may represent up to 80–90 % over the Ara and the Donga catchments (Guyot et al., 2009; Peugeot et al., 2011), it certainly represents one of these key diagnostic variables; therefore in order to achieve the overarching goal of this paper – which is to study the coupling between the subsurface dynamics, the evapotranspiration and the exchanges with the permanent groundwater – a prerequisite is to dispose of appropriate evapotranspiration measurements. This is the case for the well instrumented Nalohou hillslope (Fig. 2). This hillslope appears to be an appropriate elementary hydrological system for such a joint study of all the water balance components, since it includes a downstream riparian forest whose role on the control of the annual water budget is guessed to be so important. Beyond the surface flow which accounts for roughly 15 % of the annual rainfall a particular attention will be paid to the water distribution within the hillslope and its impact on evapotranspiration and water storage. Indeed, Guyot et al. (2009) have shown that taking into account only the water stored in the first meter of soil during the wet season is not sufficient to explain the measured actual evapotranspiration. Guyot et al. (2012) showed that during the dry season, the measured turbulent fluxes are the signature of persisting vegetation. Therefore, representing the functioning of such a hydrological system requires to use a model able to simulate both the vertical and lateral redistribution of water susceptible of replenishing the permanent deep water storage and the pumping up of this deep water by the vegetation. To that end, the physically-based Hydrus model is used here as a tool to help obtaining a proper conceptual understanding of collocated hydrological processes, model calibration being avoided as much as possible. A virtual

HESSD
10, 5643–5686, 2013

experiment is conducted – as suggested by Weiler and McDonnell (2004) – in order to test the influence of the riparian forest located downslope and of the deep permanent groundwater on the hillslope water balance.

The first section of the paper is devoted to describing the study site, the hydrological data, the studied period and the model construction. The method used to define the base case simulation is then presented in the second section, before analysing the results of the model simulations and in Sect. 3. Section 4 synthesizes these results in regard to our understanding of the hydrodynamics and to the computation of the water budget at the hillslope scale, allowing to derive a schematic of the hillslope hydrodynamics and opening a discussion for the future.

2 Material

2.1 Study site

The study site is a part of the Sudanian mesoscale site of the AMMA-CATCH observing system (Lebel et al., 2009). It is located in the upper Ouémé catchment in North-Benin, Lat 9.74° N, Long 1.60° E (14 400 km^2, Fig. 1). The upper Ouémé elevation ranges from 230 m to 620 m, with a gently inclined slope of about 3 % along the main stream. The land use is composed of four main vegetation types: cultivated area associating crop and fallows (16 %), shrub savannah (32 %), woody savannah (42 %), forest (8 %), leaving about 2 % of urbanised and free water areas (Judex et al., 2009). About 50 % of the surface is or has been cultivated, while 50 % remain practically natural. The riparian forests, even if they cover only a negligible fraction of the landscape (0.9 %) are commonly found, bordering the second and upper order streams (Séguis et al., 2011b). The hillslope studied here is entirely cultivated with crop rotation and fallows and its lower part is bordered by a riparian forest covering 5 % of our elementary hydrological unit. The rainfall regime is driven by the InterTropical Convergence Zone (ITCZ) migration, with 65 % of the annual total of 1190 mm falling during three months between

HESSD
10, 5643–5686, 2013

July and September (Le Lay and Galle, 2005) and almost no rainfall from November through March. As a consequence, rivers dry up from mid-December to June. Intermittent streamflow lasting a few days are observed, especially on small catchments, before regular rainfall starts in July after the monsoon onset, the flow becoming then permanent for 4 or 5 months. High waters occur from mid-August to the end of September, depending on the seasonal cycle of the year under consideration.

The ITCZ migration also determines the wind characteristics: the Harmattan blows dry air from the North during the dry season, while the humid wind blowing from the southern ocean characterises the wet season. The averaged daily air temperature remains around 26 °C all year long. At a monthly time step, the reference evapotranspiration ET_0 (Allen et al., 1998) shows low seasonal variability, with a maximum of 5–6 mm d^{-1} at the end of the dry season and a minimum of 3–4 mm d^{-1} in the wet season. The soils are mainly of "Ferruginous tropical leached" type (Faure and Volkoff, 1998) weathered gneiss and micaschist, fractured bedrock substratum (Affaton, 1987; Descloitres et al., 2011). The soils are closely related to the nature of parent materials but also to the topographic position: leached soils on crests and mid-slopes (lixisols), plinthisols with or without outcrops of hardpan at the slope bottom and thin sandy soils overlying a thick clayey horizon in the *bas-fonds* (Faure, 1977; Giertz and Diekkrüger, 2003). Typical depths of the horizon base are 15 to 40 cm for the A horizon, 70 to 160 cm for the B horizon, and lower for the C horizon (Faure, 1977). The A horizon is very sandy, mainly sandy loam, while the B horizon is more clayey, mainly sandy clay loam, finally, the samples from the C horizon becomes even more clayey and less sandy, mainly sandy clay and sandy clay loam as numerous tropical soils (de Condappa et al., 2008). The aquifer of the permanent and unconfined groundwater is mainly made up of silty and clayey saprolites, 5–25 m thick, overlying a metamorphic basement. Hereafter, this permanent and unconfined groundwater is called permanent groundwater. The level of the permanent groundwater table remains approximately parallel to the soil surface all year long and fluctuates between 2 m and 5 m deep (Séguis et al., 2011b).

HESSD
10, 5643–5686, 2013

2.2 Hydrological data

The studied hydrological system is a hillslope, limited upslope by the catchment boundary and downslope by the river. The upper side of the hillslope is the soil surface and the lower one is the bedrock. Various sensors are deployed in this hillslope in order to monitor the different hydrological terms (Fig. 2). One rain gauge is located on the upper part of the hillslope. Nine piezometers and three soil moisture stations are located along the hillslope. The lower soil moisture station is 40 m from the river; the middle one is located on a slope break (198 m from the river) on a crop; the upper soil moisture station is located on vegetation fallow at 508 m from the river. Each soil moisture station has five measurement depths at 10, 20, 40, 60 and 100 cm. Piezometers were installed at the same locations down to 2, 10 and 20 m deep. One flux tower (eddy correlation measurements) associated with a meteorological station is located 100 m from the mid slope station. The meteorological station includes measurements of atmospheric pressure, air temperature, relative humidity, wind speed and direction at 2 m and a complete radiation budget. One Large Aperture Scintillometer (LAS) along a 2.4 km optical path completes the experimental instrumentation. The actual evapotranspiration is deduced from LAS measurements through the computation of the energy balance at hillslope scale (1 km^2). More details on the experimental setup can be found in Guyot et al. (2009).

Soil physics properties are derived from various field measurements. The collocated water content and suction measurements are used to evaluate retention curve parameters within the two first meters. For deeper layers (from 2 to 7 m), soil samples extracted from experimental wells are used to determine the retention curve characteristics using the mercury intrusion porosimetry method (Xu et al., 1997a, b). Disk infiltrometer measurements (Robert, 2012) are used to determine the saturated hydraulic conductivities of the three soil layers (soil 1: 0–50 cm, soil 2: 50–200 cm and soil 3: 200–300 cm) down to 3 m deep. The hillslope vegetation dynamics was assessed by a composite Leaf Area Index (LAI) time series based on a combination of satellite LAI

HESSD
10, 5643–5686, 2013

products (CYCLOPE, MODIS, SEVIRI), constrained by in situ measurements derived from hemispherical photographs using the method set-up by Weiss et al. (2004).

2.3 Studied period

Hillslope hydrodynamics is analysed at the annual time scale in order to interpret the annual water budget and intra-annual variability due to contrasted water content conditions: dry season, wet season and transient periods. The studied years, 2006 and 2007 have contrasted meteorological conditions. Annual rainfall was 851 mm in 2006 (dry year) and 1218 mm in 2007 (normal year). In 2006, apart from an isolated but significant rainfall (25 mm) observed mid-February, the rainy season extends from mid-April to mid-October. In 2007 the rainy season lasts 1.5 month longer (April to mid-November). The annual dynamics of the LAI is consequently different between the two years (Fig. 3). In 2006, the LAI increases early in February, in reaction to the early rain, then it decreases slightly until May when it starts growing again steadily to reach its maximum in August. In 2007, the increase starts in March only but it is steady and regular until it peaks in July, almost one month in advance as compared to 2006. The decreasing phase of the LAI is similar in 2006 and 2007 despite a 15 days delay in 2006. The annual cycle of the reference evapotranspiration is also given for both 2006 and 2007 in Fig. 3 (11 day moving averages), showing a similar dynamics for the 2 yr.

2.4 Model construction

Given the symmetry of the topography and soil conditions transversally to the slope, the hillslope is studied as a 2-D system, as shown in Fig. 4. The finite element model Hydrus 2-D (Simunek et al., 2006) is used. This model numerically solves the Richards' equation for water flow in variably saturated porous media. Hydraulic soil properties are described with the van Genuchten–Mualem model without considering hysteresis (van Genuchten, 1980). The values of the 6 parameters used in the van Genuchten-Mualem model are presented in Table 1. The governing flow equation (Richards' equation)

HESSD
10, 5643–5686, 2013

includes a sink term S which represents the transpiration term. This process is computed using a root water uptake model described by:

$$S(h) = a(h) \cdot S_t \cdot T_p \cdot b(x,z), \tag{1}$$

with a the water stress response, function of the pressure head h; S_t the soil surface associated with transpiration; T_p the potential water uptake rate (potential transpiration) and b the normalized root water uptake distribution in horizontal (x) and vertical (z) dimensions.

A S shaped function (van Genuchten, 1987) is chosen to represent the water stress response function a:

$$a(h) = \begin{cases} \dfrac{1}{1 + \left(\frac{h}{h_{50}}\right)^p} & \text{for} \quad h > h_{wp} \\ 0 \quad \text{for} \quad h \leq h_{wp} \end{cases} \tag{2}$$

Classical values are specified for h_{50} (pressure head at which the root water uptake is reduced by 50 %: −8 m), p (exponent parameter of the water stress response function: 3) and h_{wp} (wilting point below which transpiration stops: −160 m). The surface area associated with transpiration S_t is the whole hillslope soil surface, reduced to a 1-D parameter (554 m: length from the upper limit of the catchment to the river) in this 2-D approximation. The potential evapotranspiration ET_p is partitioned into the potential evaporation (E_p) and the potential transpiration (T_p) depending on the LAI (Ritchie, 1972):

$$E_p = ET_p \cdot e^{-K \cdot LAI}$$
$$T_p = ET_p \cdot \left(1 - e^{-K \cdot LAI}\right) \tag{3}$$

Where K is the extinction coefficient of the canopy for total solar irradiance. Following López-Cedrón et al. (2008), K is prescribed equal to 0.5. This value was confirmed

HESSD
10, 5643–5686, 2013

experimentally on the study site by processing the hemispherical photographs used to estimate the LAI.

The normalized water uptake distribution $b(x,z)$ is considered as being driven by the 2-D plant root distribution, which itself is considered as binary: either there does exist plant roots and the value of the b parameter is equal to one in Eq. (1); or it does not exist and the value of the b parameter is set equal to zero (see the illustration of this distribution in Fig. 4). Besides, two types of plant root system are defined: a crop root system and a tree root system characterised by their different rooting depth. The crop root system covers the entire hillslope and, according to observations, the bulk of the roots are located above 50 cm. The tree root system is concentrated downslope, in relation to the riparian forest. The riparian forest is 20 m large but the root extent may be larger. Because it is difficult to obtain accurate observation of the tree root system, its extent is calibrated in depth and width.

The model geometry was derived from the site topography. The finite element mesh had 6219 nodes with a specified size of 0.5 m and a stretching factor of 4. Three soil layers were identified from field measurements at 0.5 m, 2 m and lower (Robert, 2012), in agreement with the typical depths of the A and B horizon base in Benin (Faure, 1977; de Condappa et al., 2008). Steady limits are assumed for the three soil layer bases throughout the hillslope, (Fig. 4). The third soil layer base is the lower boundary of the domain. It is assumed to be 7 m deep due to local observation of the bed rock. Knowing that the observed groundwater table fluctuates between 2 and 5 m deep, the lower boundary is saturated all year long. During the marked dry season, simulated suction at the soil surface is very high due to evaporation. To avoid numerical problems in this configuration, roots are removed for nodes above 20 cm depth.

An atmospheric boundary condition is specified at the surface, a no flux boundary condition at the lower boundary (Fig. 4). Concerning the upslope (respectively downslope) boundary conditions, a symmetric functioning of divergent fluxes due to the limit of the catchment (resp. convergent fluxes due to river) is assumed, resulting in a no flux condition. Next to the river, a seepage face boundary condition is prescribed, allowing

HESSD
10, 5643–5686, 2013

seepage to the river if the soil is saturated. The model initialisation takes advantage of the 4 months period without rainfall, from the last rain to the first one (November 2005 to February 2006). After three months the initial prescribed value is of low effect on the simulated water content. At the beginning of the initialization period, a uniform high water content value of 0.23 $cm^3 cm^{-3}$ is prescribed all over the domain. The model is then run for 81 days with the reference evapotranspiration as unique forcing. The study period started the 1 January 2006 based on the simulated model state. The 2007 validation simulation is initialized with the last time step of the 2006 simulation.

3 Base case simulation and virtual experiment

3.1 Model calibration and evaluation

Soil parameters were locally measured or inferred from measurements for the three soil layers. Nevertheless, given its importance in water dynamics and the local variability of the measurements, the saturated hydraulic conductivity is calibrated. The aim of the calibration is to obtain a reasonable and plausible model according to the internal dynamics. A perfect fit between all data and all model outflows is not targeted. The focus is on soil moisture and permanent groundwater to evaluate the internal dynamics and actual evapotranspiration which is the main component of the water budget. The calibrated saturated hydraulic conductivity of each soil layer is constrained to be within one order of magnitude of the measured values. The calibration quality is visually appraised. Vegetation parameters are the root depth extent of crop and trees. The crop rooting depth has been visually observed but the tree root extent is not well known since the lateral extent may be larger than the tree extent and the root depth has not been investigated below two meters deep. These parameters are calibrated by minimizing the differences between the observed and the predicted suctions at 20 and 100 cm depth and permanent groundwater table elevation at three levels of the hillslope: top, middle and bottom (Fig. 2); as suggested by Keim et al. (2006), this calibration is carried out

HESSD
10, 5643–5686, 2013

manually. The quality of the final simulation is described using the KGE performance criterion (Gupta et al., 2009) (Eq. 4) for each considered variable.

$$\mathrm{KGE} = 1 - \sqrt{(r-1)^2 + (\alpha-1)^2 + (\beta-1)^2}, \tag{4}$$

$$\alpha = \frac{\sigma_{\mathrm{sim}}}{\sigma_{\mathrm{meas}}}, \tag{5}$$

$$\beta = \frac{\mu_{\mathrm{sim}}}{\mu_{\mathrm{meas}}}, \tag{6}$$

with r, the Pearson product-moment correlation coefficient, α the ratio between the standard deviation of the simulated values (σ_{sim}) and the standard deviation of the measured values (σ_{meas}), β the ratio between the mean of the simulated values (μ_{sim}) and the mean of the measured values (μ_{meas}).

The 2006 calibrated simulation is called the base case simulation. This simulation is analysed at the daily time step, focusing on its internal hydrodynamics and its water budget. The internal dynamics of the vadose zone and the permanent groundwater table are illustrated in Fig. 5 for the middle and the bottom of the hillslope. The middle hillslope position is representative of the main part of the hillslope (without riparian forest). The bottom position is representative of the hydrodynamics functioning near the riparian forest. Being the lowest instrumented position of the hillslope, the bottom position integrates all the upslope processes. The model is then evaluated on year 2007 which is not used for calibration.

3.2 Virtual experiment modelling

A virtual experiment is performed in order to understand the role of the internal hillslope hydrodynamics in the water balance. The virtual experiment is intended at analysing the impacts of the riparian forest and of the permanent groundwater table elevation on the water budget. The virtual experiment is composed of three simulations. The base case simulation is the reference to which simulations of the virtual experiment are

HESSD
10, 5643–5686, 2013

compared. The characteristics of the 3 simulations composing the virtual experiment are detailed in Table 2.

The goal of simulation 1 is to test the impact of the presence/absence of the riparian forest on the water budget of the elementary hydrological unit. To this end, the tree root system is replaced by the crop root system (20–50 cm depth). However, the LAI time-series used in this configuration is the same as in the base case simulation, meaning that the impact on the evapotranspiration due to the modifications of the LAI when removing the riparian forest is not addressed here. This also means that the partitioning of the potential evapotranspiration between the potential evaporation and the potential transpiration, as defined by Eq. (3) is neither modified. In the end, the reduction of the actual transpiration due to the suppression of the riparian forest is proportional to the change of the plant root system distribution – as defined by the function $b(x,z)$ – when a crop is started after clearing the forest. In simulation 2 the riparian forest is maintained but the permanent groundwater is suppressed and replaced by deep drainage, which is a lost component for the system: numerically this is achieved by replacing the no flux condition at the lower boundary of the domain by a free drainage condition. In simulation 3, both the forest and the permanent groundwater are removed, allowing testing the combined effect of suppressing simultaneously these two essential components of the system.

4 Results

4.1 Base case simulation

The calibration step determines the values of 5 parameters: the saturated hydraulic conductivity for the 3 soil layers and the tree root system extent (depth and lateral extent). The others parameters are prescribed from field measurements as explained above. Soil physics parameters, whether prescribed or calibrated, are summarised in Table 1, as already mentioned earlier. The calibrated depth of the tree root system is set

HESSD
10, 5643–5686, 2013

to 4 m. The tree roots develop where moisture is available (Wan et al., 2002; Peek et al., 2006) but roots also need oxygen, and growth is restricted where oxygen is limited by the water table. Knowing that the water table level fluctuates between a depth of 2 and 5 m, the calibrated value of 4 m can be considered as realistic. The lateral extent of the tree root system is fitted as covering the first 30 m from the river which is realistically larger than the lateral extent of the riparian forest observed on the studied hillslope (20 m). In the vicinity of this hillslope, a lateral tree root has been observed 20 m from a tree. With this calibration the tree and crop root systems represent respectively 17 and 83 % of the total root system volume, while the riparian forest covers only 5 % of the surface, against 95 % for the crops.

The 2006 calibrated simulation reproduces correctly the internal dynamics of the vadose zone and of the permanent groundwater table, as can be seen from the graphs of Fig. 5 illustrating the annual evolution for the bottom and the middle of the hillslope. Figure 5a and a′, which are identical, show the measured rainfall, with an isolated rainfall in February, and the wet season from April to October. Water contents at 20 cm depth (Fig. 5b and b′) are well simulated all along the year for the two positions on the hillslope, albeit a systematic and weak underestimation (about 0.02 $m^3\,m^{-3}$) during the dry season. An underestimation also occurs during the heavy rain of September for the bottom position. Simulated water contents at 100 cm depth (Fig. 5c and c′) are in a good agreement with the measurements during the dry season. For the bottom position at 100 cm depth, the model underestimates the observed water contents of the wet season by almost 30 %. For the middle position, the base line of the water content is correctly simulated for the whole year, but three water content peaks occurring during the rainy season are missed. These peak values correspond to the temporary formation of an intermittent water table, observed in the field but which is not really simulated as such by the model because of a too weak contrast between the physical parameters of the 1st and 2nd soil layers (the saturated hydraulic conductivity of the 2nd horizon was fitted such as to correctly simulate the water transfers to the 3rd horizon). The permanent deep groundwater (Fig. 5d and d′) displays only a low frequency

HESSD
10, 5643–5686, 2013

time variation, as the high time frequencies of the atmospheric forcing are smoothed out with depth. The simulated and observed groundwater tables are markedly different on the bottom and the middle position. At the bottom position (Fig. 5d) the simulated amplitude is in good agreement with measurements but with a 2 months delay. At the middle position (Fig. 5d′) there is also a delay of the simulation, reduced to 1 month, for the minimum and the maximum; but, in addition, the simulated annual amplitude (1–3 m) is much lower than the measured one (2–6 m) and the simulated water table is about 1 m deeper than the observed one. In Fig. 6, the simulated evapotranspiration (ET) is then compared to the 2 series of observed evapotranspiration (LAS and flux tower). ET is well simulated during the wet season, almost reaching the reference evapotranspiration ET_0 much in same way as the observations do. The mean simulated evapotranspiration is about 0.5 mm d^{-1} during the dry season which is in agreement with the measurements. Moreover, evapotranspiration is correctly simulated during the transition periods: the beginning of the wet season with an isolated rain event and the decreasing at the end of the wet season.

High water velocities are located within the permanent groundwater table and they increase downslope (Fig. 7). Velocity vectors are oriented downslope and parallel to the bedrock (not shown in the figure). Within the vadose zone, velocities are small and spatially homogeneous. The spatial distribution of water velocities keeps this general structure all the year long (not shown). Consequently, in term of mass transfer, the lateral water flux is mainly provided by permanent groundwater lateral flow.

The synthetic annual water balance of the hillslope is shown in Fig. 8. Despite a rainy season that does not start until the end of April (black solid line), the cumulative transpiration starts to increase regularly at the end of January; it then increases at a larger and steady rate from the beginning of May (likely as a reaction to the installation of the rainy season) to the end of November. The cumulative annual transpiration represents 73 % of the annual rainfall. The evaporation remains low in the dry season and mainly occurs during the wet season, reaching 27 % of the annual rainfall. The seepage term remains negligible all the year long, producing no runoff. The water storage is the sum

HESSD
10, 5643–5686, 2013

of the water stored in the deep aquifer and of the water stored within the vadose zone. Change in water storage is calculated by closure of the water balance at the hillslope scale. This term can increase at daily scale in response to rainfall events (see for instance the reaction to the isolated rain event of mid-February) but globally it decreases until mid-July, because the evapotranspiration is significantly greater than rainfall during this period, pumping the missing water from the water table and depleting it. The water storage then starts to increase until the end of the rainy season; at this point it decreases again to finally get back to the zero line, the net water storage for the year 2006 being about 0.2 % of the annual rainfall. This means that during this below-than-normal rainy year, there was neither annual water storage nor seepage. At the annual time scale, evaporation plus transpiration equals rainfall.

4.2 Model evaluation

The model, fitted to the 2006 observations is evaluated on year 2007. The same variable as those used in Fig. 5 for 2006 are chosen to illustrate the simulation quality for 2007 (Fig. 9). Water contents at 20 cm depth at the bottom position (Fig. 9b) and at mid-slope (Fig. 9b′) are correctly simulated except for the end of the wet season and the transient period from the wet to the dry season. The simulated water content was lower (resp. higher) than the observed one at the bottom (resp. middle) position. Concerning water contents at 100 cm depth at the bottom position (Fig. 9c) and at mid-slope (Fig. 9c′), the annual dynamics is quite well simulated until a series of large rain events occurs at the beginning of September, the response of the model being much smoother than that of the observations. However, as for year 2006, the model does not achieve to simulate the end of the wet season and the transient period from the wet to the dry season. At mid-slope, the simulated water content reaches the measured maximal water content value at the end of September. This value close to the saturated water content is in accordance with measurements but high frequency fluctuations are missing and all in all, the maximum is reached too late. The KGE performance criterion is similar in calibration (2006) and evaluation (2007) years for water content at 20 cm

HESSD
10, 5643–5686, 2013

and 100 cm. The level of the permanent groundwater table at mid-slope (Fig. 9d′) is well reproduced, the annual fluctuation being correct in both timing and magnitude. For this variable, the evaluation year is better simulated than the calibration one and the KGE criterion is higher in 2007 than in 2006 (0.58 against 0.45). The simulated values of the level of the permanent groundwater table at the bottom position are reasonably good during the first part of the year. After rising rapidly in August, the observed level of the permanent aquifer at the bottom of the slope reaches a plateau in September and remains stable until December (Fig. 9d); this behaviour is well captured by the model except that the plateau is largely overestimated in the simulation, consequently lowering the KGE criterion in 2007. The fact that the simulated level reaches −3 m in 2007 against −5 m in 2006 certainly results from 2007 being much wetter than 2006 (1218 mm against 851 mm). On the other hand, the observations display a much weaker interannual variability of the groundwater level at this particular position (bottom of the slope), which suggests a buffer effect in the dynamics of this permanent deep groundwater, probably related to the 3-D structure of the aquifer at larger scale. By construction this larger scale 3-D structure is not captured in our model and addressing this issue is out of the scope of this paper.

Overall, although the Hydrus 2-D simulations did not perfectly reproduce the behaviour of the soil water and water fluxes within the experimental hillslope, the simplified hillslope representation obtained through the calibration responds correctly to the atmospheric forcing for the two different years. Even though some fine tuning of the calibrated parameters could improve the simulation for 2007, our ultimate goal is not to obtain a perfect representation of a single hillslope – which would certainly be an unrealistic dream given the complexity of these simulations, but rather to dispose of an acceptable test bed for setting up a virtual experiment on how the vegetation and the deep aquifer interact and control the water budget.

HESSD
10, 5643–5686, 2013

4.3 Virtual experiment: impacts of riparian forest and permanent groundwater on evapotranspiration

The virtual experiment bears on year 2006. In simulation 1, the absence of riparian forest results in a reduction of the annual transpiration from 625 mm to 498 mm, while evaporation remains constant (Table 3). The hillslope generates seepage all the year long (not shown), and represents 13 % of the annual rainfall. The absence of the permanent groundwater (simulation 2) reduces the annual transpiration to 443 mm. The evaporation (226 mm) is very close to the value of the base case simulation (229 mm) and seepage is negligible as in the base case simulation. For simulation 3 (no riparian forest, no permanent groundwater), the annual evaporation slightly decreases to 215 mm (accounting for 25 % of annual rainfall), seepage being also negligible. The annual transpiration decreases to 472 mm, a value close to that of simulation 1 and 2, although there is neither riparian forest nor groundwater.

By construction, the potential evaporation, which is time-dependent, is the same for all the simulations. The annual evaporation is nearly similar for all the simulations and accounts for 25 to 27 % of the annual rainfall. The negligible variation of evaporation between the simulations with and without permanent groundwater suggests a very weak impact of the permanent groundwater on the annual evaporation. In the same way, the negligible variation in evaporation between the simulations with and without riparian forest shows a very weak impact of the tree root system on the annual evaporation.

5 Synthesis and conclusions

5.1 Position of the problem: addressing the links between evapotranspiration and permanent groundwater

As they transpire water into the atmosphere even during the dry season, it is assumed that forests with perennial leaves play an important role in the dynamics of the West

HESSD
10, 5643–5686, 2013

African monsoon, especially during its onset. In order to penetrate deep into the continent, a healthy monsoon may use this continental source of humidity to relay the water vapour originating from the ocean. Of course, for this mechanism to operate, water storage must be available sufficiently deep in the soil so that the tree roots can pump it into the atmosphere even when the top soil layers are totally dry a few weeks after the end of the rainy season. In order to represent correctly the water cycle at seasonal and annual scales, and how it interacts with the climate dynamics through the water budget, it is thus of outmost importance that models incorporate a representation of the coupling between the evapotranspiration and the water storage in the permanent aquifer, the table level of which fluctuates between 2 and 5 m. While it is intended to use such models at meso to regional scale, a previous attempt at modelling the water budget at this scale, using a reparametrized version of Topmodel calibrated against the observed discharges of the Donga River (586 km^2), proved to be unsuccessful: in order to reproduce correctly the observations, a fictive lost water component had to be added, meaning that the actual evapotranspiration was not captured correctly. It was thus decided in the work presented here to explore, on a small and well instrumented hydrological unit, how the coupling between the evapotranspiration and the deep water storage operates – where and when the trees are extracting water from deep groundwater – and which proportion of the water budget it controls. This is done by running a physical 2-D-model able to represent the dynamical equilibrium between vertical water input (rainfall) and its lateral distribution. This 2-D approach is justified (i) by the overall symmetry of this elementary unit transversally to the slope and (ii) by the difficulty of implementing a comprehensive 3-D instrumentation required to document the spatial variability of all the parameters needed to run a 3-D model.

5.2 Riparian forest and permanent groundwater: a coupled transpiration system

Depending on years, evapotranspiration represents between 80 % and 90 % of the annual water budget in this region. A first important result obtained when running Hydrus

HESSD
10, 5643–5686, 2013

2-D on our elementary hydrological unit is its ability to retrieve correctly the annual cycle of the evapotranspiration and its corresponding annual total, using soil parameters and root depths observed in the field (base case simulation). The permanent groundwater dynamics is also correctly simulated, implying that the water transfer between the soil and the atmosphere at the hillslope scale is well captured by the model. The ability of simulating properly the seasonal dynamics of the permanent groundwater is also an important point since these aquifers may produce a significant contribution to regional river flows after the end of the rainy season.

Further exploring how the transpiration from the riparian forest is related to the groundwater was done through a virtual experiment, summarised in Table 3, where two paths are considered to move from the base state simulation to a state where both the riparian forest and the permanent aquifer are removed (simulation 3), producing a 153 mm reduction of the annual transpiration. In the first path, the riparian forest is removed first, resulting in a 127 mm decrease of the annual transpiration; removing next the permanent groundwater produces an additional decrease of 26 mm. The second way is to first remove the permanent groundwater, involving a 182 mm decrease of the annual transpiration, and then the riparian forest, resulting in a slight increase in transpiration (29 mm). This slight increase is not so significant but still deserves some explanation. It basically means that in simulation 3 the annual transpiration is higher than in simulation 2 despite a lower potential transpiration (smaller total root system volume). However, the additional roots in simulation 2 are located deep in the soil (riparian forest root system); in a configuration where the deep permanent aquifer was removed, these roots have no water available for extracting it. On the other hand, in simulation 3, there are more roots in the upper layers of the soil (crop root system) where they can extract rapidly the water available from the rainfall infiltration. In other words, in a configuration where there is no permanent deep water, a crop root system is more efficient than a riparian forest root system to extract water from the soil. To summarise, path 1 (suppressing the forest first, then the aquifer) shows that the transpiration of the riparian forest drives the groundwater depletion, whereas path 2 shows

HESSD
10, 5643–5686, 2013

that the deep groundwater is necessary to supply the riparian transpiration system: the riparian forest and the deep groundwater form a coupled transpiration system.

5.3 Intra-annual variability of the transpiration sources

The riparian forest transpiration due to the deep root system (0.5–4 m) is assumed to be equal to the difference between the transpiration of the base case simulation and that of simulation 3. Thus the riparian transpiration is 153 mm or 37 % of the total hillslope transpiration (Fig. 10), even though the riparian forest represents only 5 % of the hillslope surface and 17 % of the total plant root system volume. Hence, the riparian forest deep root system is a more efficient transpiration system than the crop root system. The same comparison is made for the wet and the dry seasons considered separately. During the wet season, the contribution of the riparian forest to the total transpiration is 19 %. This value is close to the proportion of the forest root volume in the whole root system. Thus, when not limited by soil water, crops and riparian forest have roughly the same transpiration efficiency. On the opposite, during the dry season, the upper soil layers are dry and the forest transpiration reaches 57 % of the total hillslope transpiration, meaning that the riparian forest is almost 6.5 times more efficient than the other vegetation in pumping water back to the atmosphere.

The riparian forest transpiration from deep soil layers (0.5–4 m) is relatively constant all along the year with an averaged value of 0.41 $mm\,d^{-1}$ at the hillslope scale (0.46 $mm\,d^{-1}$ during the wet season and 0.37 $mm\,d^{-1}$ during the dry season). It is the signature of deep rooted persistent vegetation in this area. Conversely, the superficial layer (0–0.5 m) shows a highly variable transpiration rate, depending on rainfall input, atmosphere demand and soil moisture availability and is consequently season-dependent. The annual transpiration signal can be interpreted as the addition of a practically constant riparian forest transpiration which is around 0.4 $mm\,d^{-1}$ at hillslope scale and a time-dependent crop transpiration which is linked to rainfall inputs. Consequently, transpiration is mainly supplied by the riparian forest during the dry season

HESSD
10, 5643–5686, 2013

and by the crops during the wet season – since the forest area represents only 5 % of the total vegetated surface.

5.4 Riparian forest transpiration explains the independence between the deep groundwater table and the river

There is another important consequence of the coupled functioning of the riparian forest and of the permanent aquifer: the forest transpiration depletes the groundwater table at such a level that it cannot contribute to the river flow. This is evidenced by comparing the significant seepage (13 % of the annual rainfall) produced by simulation 1 (absence of riparian forest) to the absence of seepage produced in the base case simulation. This significant seepage is produced by the rise of the simulated permanent groundwater table above the river bed (not shown). Since these 2 simulations differ only by the absence/presence of the riparian forest, this suggests that when the riparian forest is removed, the groundwater table rises to a level allowing it to feed the flow in the river bed. The same conclusion stems from the comparison of simulation 1 to simulation 3 (differing only by the presence/absence of the groundwater level); the riparian forest being absent in both cases, the absence of seepage in simulation 3 means that the seepage obtained in simulation 1 is produced by the permanent groundwater. These results suggest that the transpiration of the riparian forest results in the disconnection of the aquifer from the river streamflow, a feature already assumed by Séguis et al. (2011b) on the Donga catchment, who roughly estimated the evapotranspiration rate required to maintain this disconnection to be in the order of 6 to 34 $mm\,d^{-1}$. Our study demonstrates that the main reason of this disconnection is the riparian forest transpiration emptying the downslope water table. However, it is possible that at the scale of a larger catchment (such as the Donga), the evapotranspiration during the dry season is not limited to the riparian forest.

HESSD
10, 5643–5686, 2013

5.5 Overall schematic of the present hillslope hydrodynamics and implication for the future

The schematic of the hillslope hydrodynamics can be summarised as follows. During the dry season (Fig. 11a), only capillary effects and weak evaporation take place along the hillslope due to the absence of rainfall events. The permanent groundwater provides lateral saturated flows which enables riparian forest transpiration. During the wet season (Fig. 11b), rainfall infiltrates. This water is available for evaporation, crop transpiration and water distribution along the hillslope or deep percolation. This last process feeds the permanent aquifer. It flows laterally downslope and provides water to the riparian forest transpiration. In both seasons, the riparian forest transpiration is supplied by the permanent groundwater, which is disconnected from the river. One uncertainty remains regarding seepage generation. The model is not producing seepage, either due to the absence of shallow groundwater level in the simulations, or simply because the studied hillslope actually does not generate seepage downslope. In this case, it has to be hypothesized that the streamflow generation takes place in other locations of the watershed.

The virtual experiment also teaches us something about the future. It shows that if the riparian forest were cut, the river flow would increase, because the downslope water table could rise until it seeps into the river. But what would happen for a hillslope covered by forest? Having shown that crop and trees have a similar transpiration rate during the rainy season leads to assume that on a forested hillslope, the transpiration is equal or only slightly higher than on a cultivated one. Thus, to a first approximation if a slope forest were cut, at the exclusion of the riparian forest, there would be little change in the water flow regime. On the opposite, if the riparian forest were cut as well, this could increase the river flow. The riparian area thus appears as a key factor for river flow supply. This conclusion may serve as a guide for land management in a context of rapid and drastic evolution of the vegetation cover. Forests are currently covering 50 % of the upper Ouémé basin and the region is witnessing a strong increase of population

HESSD
10, 5643–5686, 2013

through inner growth and settlement from outer areas, involving land clearing; whether this clearing occurs with or without cutting the downslope riparian forest, might consequently have a strong impact on the local water cycle, and, regionally, to the monsoon dynamics.

5.6 Future research

In order to obtain mesoscale hydrological models that are relevantly parametrized to be run in interaction with regional climate models in the Soudanian climate sub-region of West Africa, investigations should continue along three main lines, spanning a hierarchy of scales.

First, the ability of a 2-D physical model to account for the main coupling processes between soil water and evapotranspiration at the hillslope scale makes it an important tool for water resource management at the interannual and local scales. However, a better identification of the local areas where soil moisture excess is producing seepage remains needed for finely representing the intra-seasonal fluctuations of the river flow at the outlet of small catchments. This production is likely limited to particular places of the basin like the *bas-fonds*. Finding a way of introducing this process in a Hydrus-like model is probably not of great significance for mesoscale models (see below), but it remains an interesting challenge from a methodological point of view. Also, note that observed temporal shallow groundwater tables are appearing synchronously with high water content peaks also observed at 100 cm depth (Figs. 5c′ and 9c′) but the relationship between these two variables is definitely not simple and deserves further analysis.

Secondly and as mentioned earlier in the discussion, it is possible that at the scale of a larger catchment (such as the Donga), the evapotranspiration during the dry season is not limited to the riparian forest. This is obviously a question that should be addressed by appropriate field campaigns in order to obtain a better knowledge of the detailed functioning of mesoscale catchments and to pondering how to introduce this additional source of dry season evapotranspiration, if it is proved that it does exist.

HESSD
10, 5643–5686, 2013

The last and most important line of investigation remains however to find a way of taking correctly into account the interactions between the deep permanent groundwater table and the riparian forest transpiration in mesoscale hydrological models, typically used for simulating the water budget of catchments covering a dozen thousands of km^2 such as the upper Ouémé (14400 km^2).

Acknowledgements. This research was funded by IRD and INSU in the framework of the AMMA program. Based on a French initiative, AMMA was developed by an international scientific group and funded by a large number of agencies, especially from Africa, European Community, France, UK and USA. More information on the scientific coordination and funding is available on the AMMA International web-site: http://www.amma-international.org. The AMMA-CATCH observing system has been funded since 2001 by IRD, INSU and the French Ministry of Research: http://www.amma-catch.org/ in cooperation with Direction Générale de l'Eau (DG-Eau) of Benin. The article processing charges have been funded by INSU-CNRS. The authors wish to particularly thank the researchers and students who helped them during the different steps of this work: T. Lebel, C. Legout, I. Zin, D. Robert, S. Soubeyran, B. Hector, M. Wubda, and the Beninese technicians T. Ouani S. Afouda for their permanent supports in the field.

The publication of this article is financed by CNRS-INSU.

References

Affaton, P.: Le bassin des Volta (Afrique de l'Ouest): une marge passive, d'âge protérozoïque supérieur, tectonisée au panafrican (600 + −50 Ma), Ph.D. Thesis, University of Aix-Marseille 3, France, 1987.

Allen, R., Pereira, L. S., Raes, D., and Smith, M.: Crop evapotranspiration?: guidelines for computing crop water requirements, Irrig. and Drain. Paper no. 56, United Nations Food and Agriculture Organization, Rome, Italy, 300 pp., 1998.

Beven, K. J.: TOPMODEL: a critique, Hydrol. Process., 11, 1069–1085, 1997.

Beven, K. J.: Calibration, validation and equifinality in hydrological modelling: a continuing discussion. . . , in: Model Validation: Perspectives in Hydrological Science, edited by: Anderson, M. G. and Bates, P. D., 43–55, J. Wiley, Chichester, New York, 2001.

Beven, K. J. and Kirby, M. J.: A physically based, variable contributing area model of basin hydrology, Hydrolog. Sci. J., 24, 43–69, 1979.

Chevallier, P. and Planchon, O.: Hydrological processes in a small humid savanna basin (Ivory Coast), J. Hydrol., 151, 173–191, 1993.

de Condappa, D., Galle, S., Dewandel, B., and Haverkamp, R.: Bimodal zone of the soil textural triangle: common in tropical and subtropical regions, Soil Sci. Soc. Am. J., 72, 33–40, 2008.

Descloitres, M., Séguis, L., Legchenko, A., Wubda, M., Guyot, A., and Cohard, J.-M.: The contribution of MRS and resistivity methods to the interpretation of actual evapo-transpiration measurements: a case study in metamorphic context in north Bénin, Near Surf. Geophys., 9, 187–200, 2011.

Faure, P.: Carte Pédologique de Reconnaissance au 1/200 000e, Feuille de Djougou, Orstom editions, Paris, France, 1977.

Faure, P. and Volkoff, B.: Some factors affecting regional differentiation of the soils in the Republic of Benin (West Africa), Catena, 32, 281–306, 1998.

Fontaine, B., Philippon, N., and Camberlin, P.: An improvement of June–September rainfall forecasting in the Sahel based upon region April–May moist static energy content (1968–1997), Geophys. Res. Lett., 26, 2041–2044, 1999.

Giertz, S. and Diekkrüger, B.: Analysis of the hydrological processes in a small headwater catchment in Benin (West Africa), Phys. Chem. Earth, 28, 1333–1341, 2003.

Giertz, S., Diekkrüger, B., and Steup, G.: Physically-based modelling of hydrological processes in a tropical headwater catchment (West Africa) – process representation and multi-criteria validation, Hydrol. Earth Syst. Sci., 10, 829–847, doi:10.5194/hess-10-829-2006, 2006.

Gupta, H. V., Kling, H., Yilmaz, K. K., and Martinez, G. F.: Decomposition of the mean squared error and NSE performance criteria: implications for improving hydrological modelling, J. Hydrol., 377, 80–91, 2009.

Guyot, A., Cohard, J.-M., Anquetin, S., Galle, S., and Lloyd, C. R.: Combined analysis of energy and water balances to estimate latent heat flux of a sudanian small catchment, J. Hydrol., 375, 227–240, 2009.

Guyot, A., Cohard, J.-M., Anquetin, S., and Galle, S.: Long-term observations of turbulent fluxes over heterogeneous vegetation using scintillometry and additional observations: a contribution to AMMA under Sudano-Sahelian climate, Agr. Forest Meteorol., 154–155, 84–98, 2012.

Judex, M., Thamm, H.-P., and Menz, G.: Utilisation des Terres et Occupation du Sol Dans le Centre du Bénin, in IMPETUS Atlas du Bénin. Résultats de Recherche 2000–2007, edited by: Judex, M., Thamm, H.-P., Röhrig, J., and Schulz, O., Département de Géographie, Université de Bonn, Allemagne, 85–86, 2009.

Kamagaté, B., Séguis, L., Favreau, G., Seidel, J.-L., Descloitres, M., and Affaton, P.: Hydrological processes and water balance of a tropical crystalline bedrock catchment in Bénin (Donga, upper Ouémé River), C. R. Geosci., 339, 418–429, 2007.

Keim, R. F., Tromp-van Meerveld, H. J., and McDonnell, J. J.: A virtual experiment on the effects of evaporation and intensity smoothing by canopy interception on subsurface stormflow generation, J. Hydrol., 327, 352–364, 2006.

Lafforgue, A.: Etude Hydrologique des Bassins Versants de Sakassou: Côte d'Ivoire, 1972–1977, Orstom editions, Paris, 1982.

Le Lay, M. and Galle, S.: Seasonal cycle and interannual variability of rainfall at hydrological scales. The West African monsoon in a Sudanese climate, Hydrolog. Sci. J., 50, 509–524, 2005.

Le Lay, M., Saulnier, G.-M., Galle, S., Séguis, L., Métadier, M., and Peugeot, C.: Model representation of the Sudanian hydrological processes: Application on the Donga catchment (Benin), J. Hydrol., 363, 32–41, 2008.

Lebel, T. and Ali, A.: Recent trends in the Central and Western Sahel rainfall regime (1990–2007), J. Hydrol., 375, 52–64, 2009.

Lebel, T., Cappelaere, B., Galle, S., Hanan, N., Kergoat, L., Levis, S., Vieux, B., Descroix, L., Gosset, M., Mougin, E., Peugeot, C., and Séguis, L.: AMMA-CATCH studies in the Sahelian region of West-Africa: an overview, J. Hydrol., 375, 3–13, 2009.

López-Cedrón, F. X., Boote, K. J., Piñeiro, J., and Sau, F.: Improving the CERES-Maize model ability to simulate water deficit impact on maize production and yield components, Agron. J., 100, 296–307, 2008.

Masiyandima, M. C., van De Giesen, N., Diatta, S., Windmeijer, P. N., and Steenhuis, T. S.: The hydrology of inland valleys in the sub-humid zone of West Africa: rainfall-runoff processes in the M'bé experimental watershed, Hydrol. Process., 17, 1213–1225, 2003.

Peek, M. S., Leffler, A. J., Hipps, L., Ivans, S., Ryel, R. J., and Caldwell, M. M.: Root turnover and relocation in the soil profile in response to seasonal soil water variation in a natural stand of Utah juniper (Juniperus osteosperma), Tree Physiol., 26, 1469–1476, 2006.

Peugeot, C., Guichard, F., Bock, O., Bouniol, D., Chong, M., Boone, A., Cappelaere, B., Gosset, M., Besson, L., Lemaître, Y., Séguis, L., Zannou, A., Galle, S., and Redelsperger, J.-L.: Mesoscale water cycle within the West African Monsoon, Atmos. Sci. Lett., 12, 45–50, 2011.

Peugeot, C., Bock, O., Boone, A., Cappelaere, B., Gosset, M., Meynadier, R., Seguis, L., Lebel, T., and Redelsperger, J.-L.: Le cycle de l'eau dans le système de mousson d'Afrique de l'Ouest, La Météorologie, Spécial AMMA, 55–63, 2012.

Philippon, N. and Fontaine, B.: The relationship between the Sahelian and previous 2nd Guinean rainy seasons: a monsoon regulation by soil wetness?, Ann. Geophys., 20, 575–582, doi:10.5194/angeo-20-575-2002, 2002.

Ritchie, J. T.: Model for predicting evaporation from a row crop with incomplete cover, Water Resour. Res., 8, 1204–1203, 1972.

Robert, D.: Caractérisation et modélisation de la dynamique de l'évapotranspiration en Afrique soudanienne en zone de socle, Ph.D. Thesis, Université de Grenoble, France, 2012.

Séguis, L., Boulain, N., Cappelaere, B., Cohard, J. M., Favreau, G., Galle, S., Guyot, A., Hiernaux, P., Mougin, E., Peugeot, C., Ramier, D., Seghieri, J., Timouk, F., Demarez, V., Demarty, J., Descroix, L., Descloitres, M., Grippa, M., Guichard, F., Kamagaté, B., Kergoat, L., Lebel, T., Le Dantec, V., Le Lay, M., Massuel, S., and Trichon, V.: Contrasted land-surface processes along the West African rainfall gradient, Atmos. Sci. Lett., 12, 31–37, 2011a.

Séguis, L., Kamagaté, B., Favreau, G., Descloitres, M., Seidel, J.-L., Galle, S., Peugeot, C., Gosset, M., Le Barbé, L., Malinur, F., Van Exter, S., Arjounin, M., Boubkraoui, S., and

HESSD
10, 5643–5686, 2013

Wubda, M.: Origins of streamflow in a crystalline basement catchment in a sub-humid Sudanian zone: the Donga basin (Benin, West Africa), J. Hydrol., 402, 1–13, 2011b.
Simunek, J., van Genuchten, M. T., and Sejna, M.: The HYDRUS software package for simulating two- and three-dimensional movement of water, heat, and multiple solutes in variably-saturated media, Technical Manual, PC-Progress, Prague, Czech Republic, 2006.
Tromp-van Meerveld, I., and Weiler, M.: Hillslope dynamics modeled with increasing complexity, J. Hydrol., 361, 24–40, 2008.
van Genuchten, M. T.: A closed-form equation for predicting the hydraulic conductivity of unsaturated soils, Soil Sci. Soc. Am. J., 44, 892–898, 1980.
van Genuchten, M. T.: A numerical model for water and solute movement in and below the root zone, Research Report, US Salinity laboratory, USDA, Riverside, California, 1987.
Wan, C., Yilmaz, I., and Sosebee, R. E.: Seasonal soil–water availability influences snakeweed root dynamics, J. Arid Environ., 51, 255–264, 2002.
Weiler, M. and McDonnell, J. J.: Virtual experiments: a new approach for improving process conceptualization in hillslope hydrology, J. Hydrol., 285, 3–18, 2004.
Weiss, M., Baret, F., Smith, G. J., Jonckheere, I., and Coppin, P.: Review of methods for in situ leaf area index (LAI) determination: Part II. Estimation of LAI, errors and sampling, Agr. Forest Meteorol., 121, 37–53, 2004.
Xu, K., Daian, J., and Quenard, D.: Multiscale structures to describe porous media Part I: Theoretical background and invasion by fluids, Transport Porous Med., 26, 51–73, 1997a.
Xu, K., Daian, J.-F., and Quenard, D.: Multiscale structures to describe porous media Part II: Transport properties and application to test materials, Transport Porous Med., 26, 319–338, 1997b.

HESSD
10, 5643–5686, 2013

Table 1. Soil physics parameters used in the van Genuchten–Mualem model for the 3 soil layers. θ_r: residual water content; θ_s: saturated water content; h_g: inflection point pressure; n: pore size distribution parameter; Ks: saturated hydraulic conductivity; L: pore conductivity parameter.

	Retention curve parameters				Hydraulic conductivity curve parameters	
Variable	θ_r [$m^3 m^{-3}$]	θ_s [$m^3 m^{-3}$]	h_g [m]	n [–]	Ks [$m s^{-1}$]	L [–]
Status	prescribed	prescribed	prescribed	prescribed	calibrated	prescribed
Soil 1	0.025	0.35	−0.50	1.8	5.2×10^{-5}	0.5
Soil 2	0.090	0.35	−0.28	1.6	3.5×10^{-5}	0.5
Soil 3	0.025	0.25	−1.00	1.8	1.4×10^{-5}	0.5

HESSD
10, 5643–5686, 2013

Table 2. Characteristics of the base case simulation and virtual experiment simulations.

	Presence of riparian forest	Absence of riparian forest
Presence of deep groundwater	Base case simulation $T_p(t) = T_{p,base}(t)$ PRSD[a]: Crop plant, tree LBC[b]: No flux	Simulation 1 $T_p(t) = 0.83T_{p,base}(t)$ PRSD: Crop plant, no tree LBC: No flux
Absence of deep groundwater	Simulation 2 $T_p(t) = T_{p,base}(t)$ PRSD: Crop plant, tree LBC: Free drainage	Simulation 3 $T_p(t) = 0.83T_{p,base}(t)$ PRSD: Crop plant, no tree LBC: Free drainage

[a] Plant Root System Distribution,
[b] Lower Boundary Condition.

HESSD
10, 5643–5686, 2013

Table 3. Summary of the annual output fluxes of the base case simulation and of the 3 simulations composing the virtual experiment.

	Presence of riparian forest			Absence of riparian forest		
		Annual value	% annual rainfall		Annual value	% annual rainfall
	Base case simulation			Simulation 1		
Presence of deep groundwater	Evaporation	229 mm	27 %	Evaporation	231 mm	27 %
	Transpiration	625 mm	73 %	Transpiration	498 mm	59 %
	Seepage	ε	–	Seepage	114 mm	13 %
	Simulation 2			Simulation 3		
Absence of deep groundwater	Evaporation	226 mm	27 %	Evaporation	215 mm	25 %
	Transpiration	443 mm	52 %	Transpiration	472 mm	55 %
	Seepage	ε	–	Seepage	ε	–

HESSD
10, 5643–5686, 2013

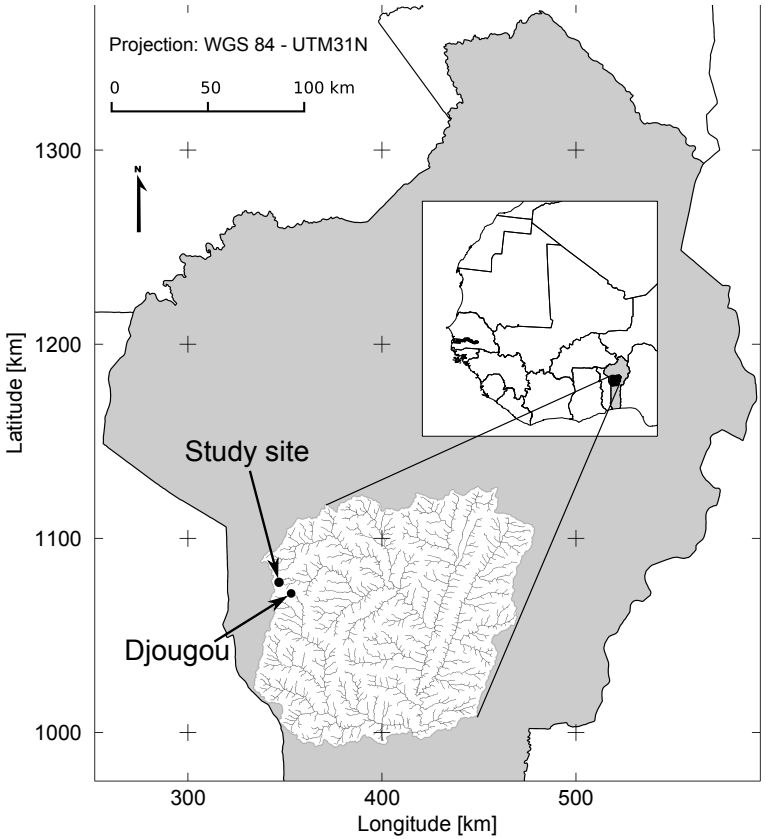

Fig. 1. Location of the study site. The watershed is the Sudanian climate mesoscale site of the AMMA-CATCH observing system, North Benin, West Africa. Republic of Benin is the grey area.

HESSD
10, 5643–5686, 2013

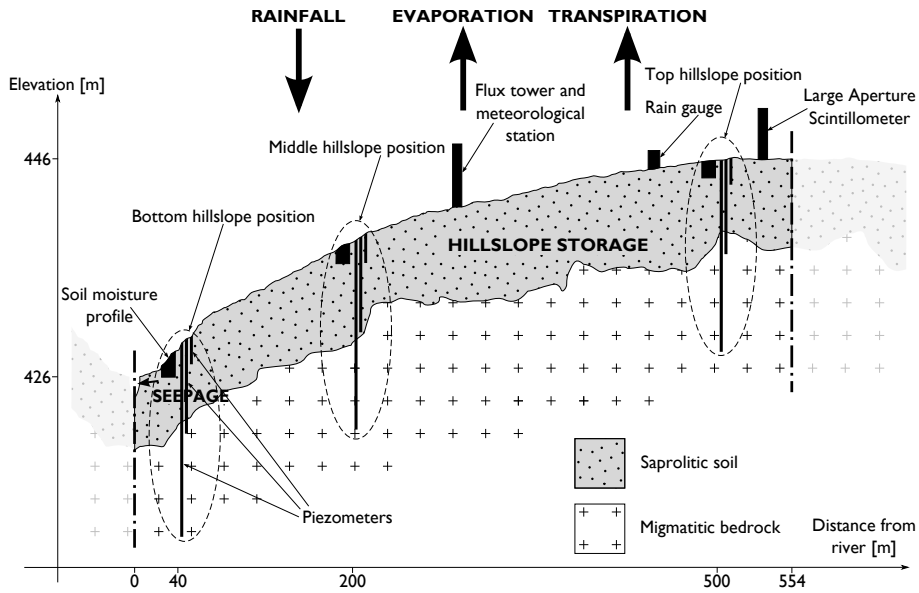

Fig. 2. Schematic hillslope representation (fluxes, water storage, available hydrologic sensors), assuming two axes of symmetry: the river downslope and the upper limit of the watershed upslope. Vertical exaggeration by a factor 10.

HESSD
10, 5643–5686, 2013

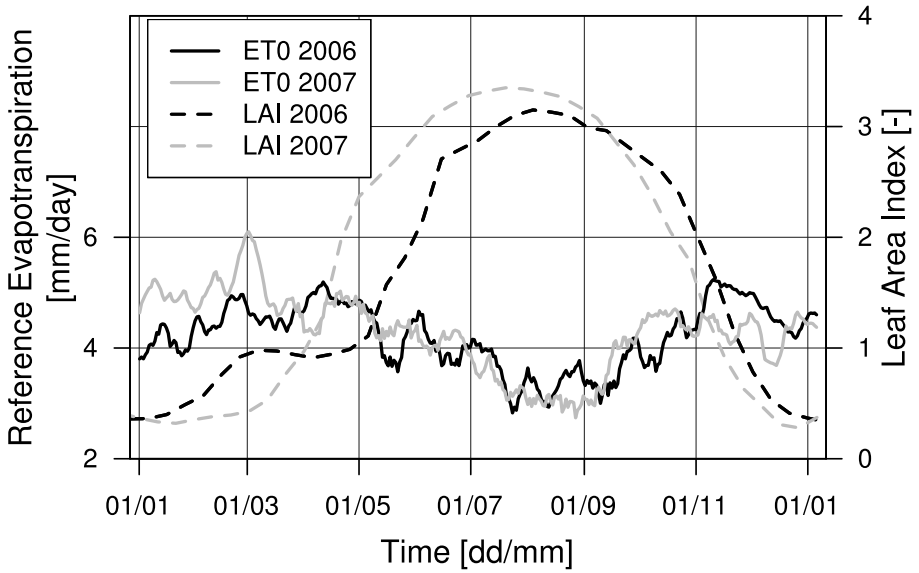

Fig. 3. Annual cycle of the reference evapotranspiration ET_0 (11 day moving average filter, solid lines) and of the Leaf Area Index LAI (averages from a composite of satellite products, dashed lines) for 2006 (black lines) and 2007 (grey lines).

HESSD
10, 5643–5686, 2013

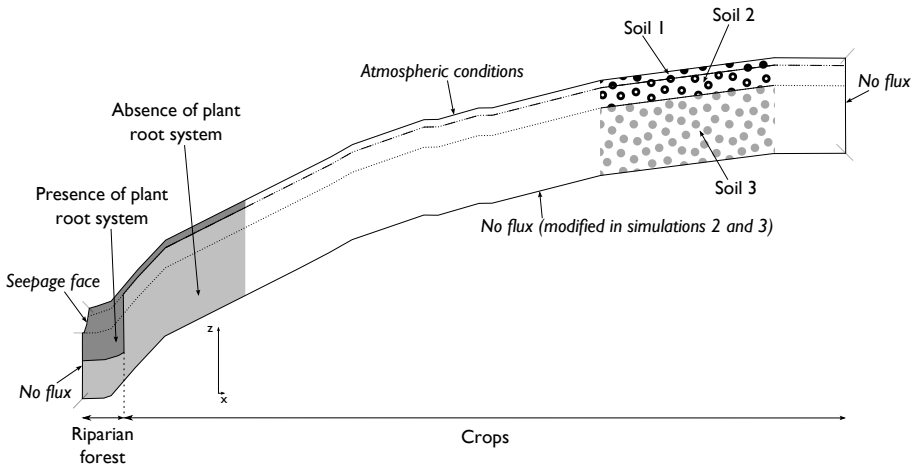

Fig. 4. Schematic of the plant root system distribution and of the soil distribution with indication of the boundary conditions. Left, plant root system distribution: the vertical dashed line downslope shows the lateral extent of the tree root system, fitted to 30 m (5 % of the hillslope length), while the long dashed lines show the continuation of the plant root system distribution upslope. Right, schematic of the 3-layer soil distribution with dotted lines showing its continuation upslope and downslope. Boundary conditions are indicated in italics. Short grey segments separate different boundary conditions. Vertical exaggeration: 10.

HESSD
10, 5643–5686, 2013

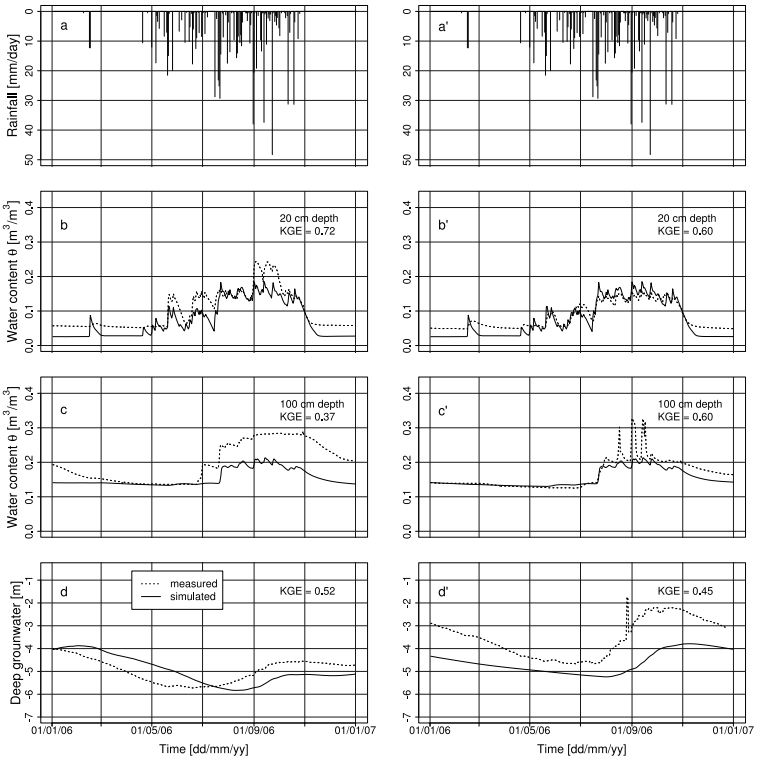

Fig. 5. Forcing variable (rainfall) and state variables of Hydrus 2-D for the base case simulation in 2006. Graphs on the left are for the bottom of the hillslope; graphs on the right are for the middle of the hillslope. **(a, a′)** measured rainfall; **(b, b′)** measured and simulated water content at 20 cm depth; **(c, c′)** measured and simulated water content at 100 cm depth; **(d, d′)** measured and simulated level of the groundwater table.

HESSD
10, 5643–5686, 2013

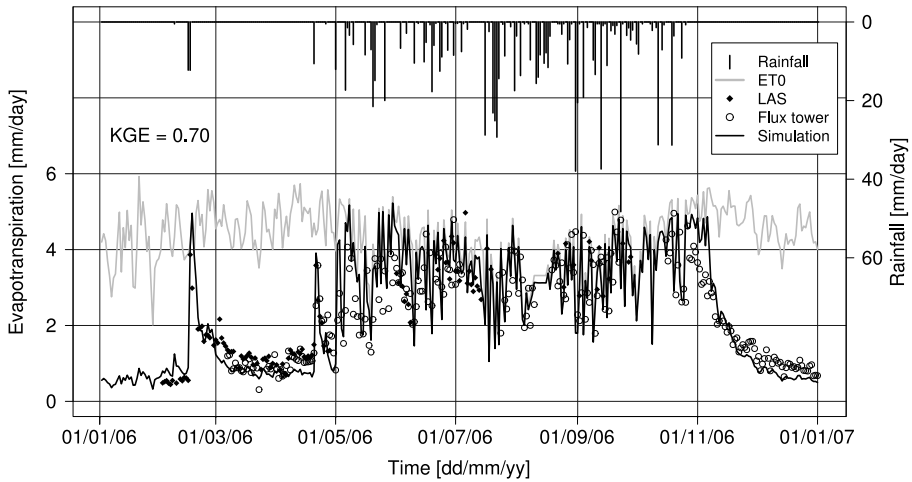

Fig. 6. Simulated and observed evapotranspiration, averaged over the elementary hydrological unit, for year 2006.

HESSD
10, 5643–5686, 2013

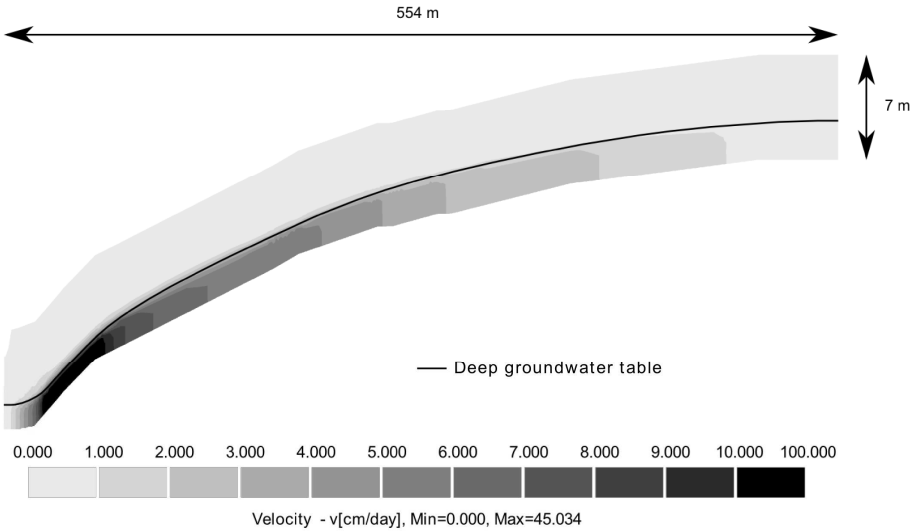

Fig. 7. Water velocity within the hillslope. The black solid line corresponds to the deep groundwater table. Day of year: 210 (29 July 2006). Vertical exaggeration: 10.

HESSD
10, 5643–5686, 2013

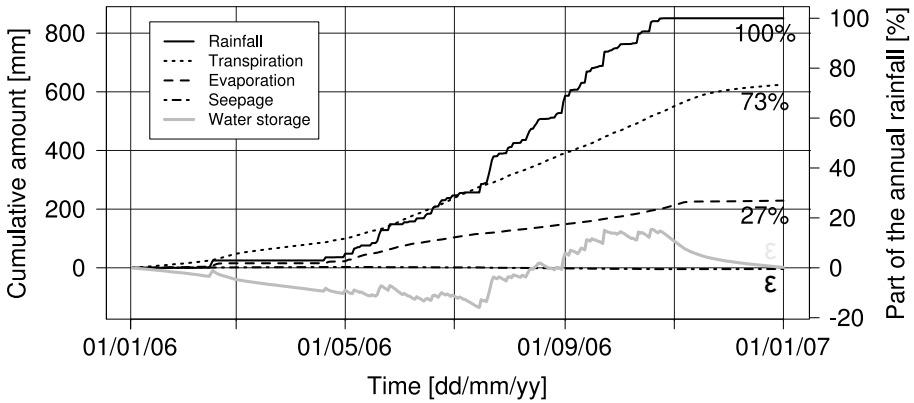

Fig. 8. Synthetic annual water balance of the hillslope: rainfall, transpiration, evaporation, seepage and water storage. All terms are simulated except the rainfall which is measured.

HESSD
10, 5643–5686, 2013

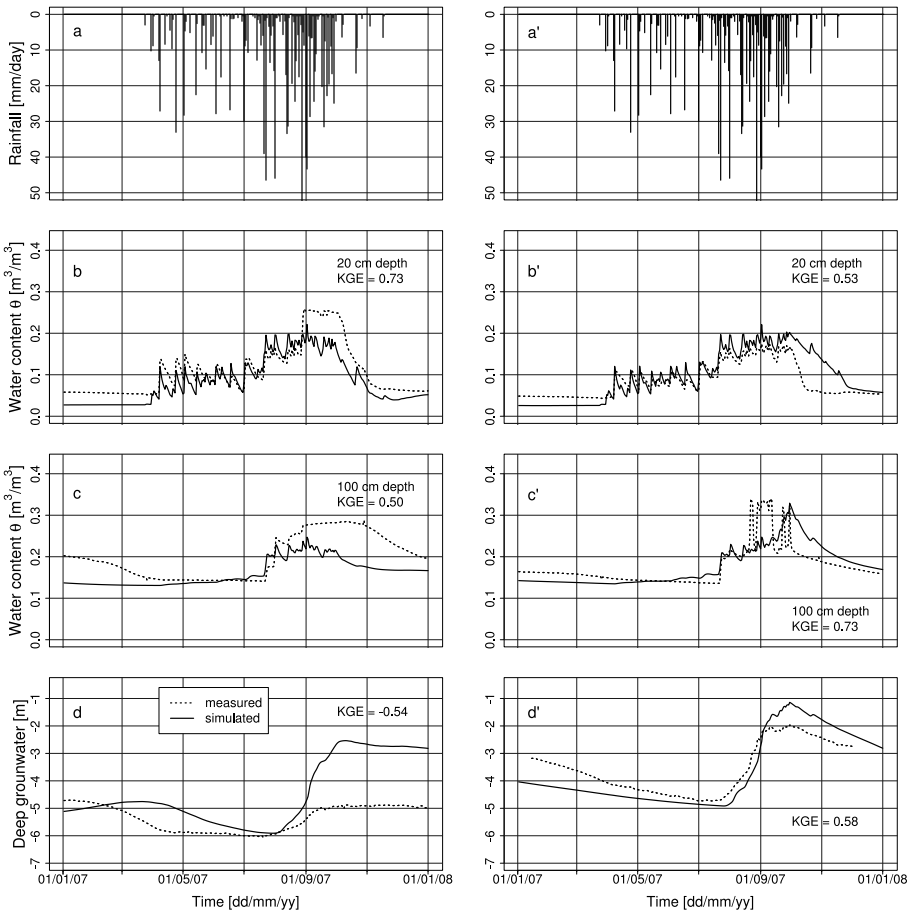

Fig. 9. Same as in Fig. 5, except for 2007 (bottom location at the left and mid-slope location at the right).

HESSD
10, 5643–5686, 2013

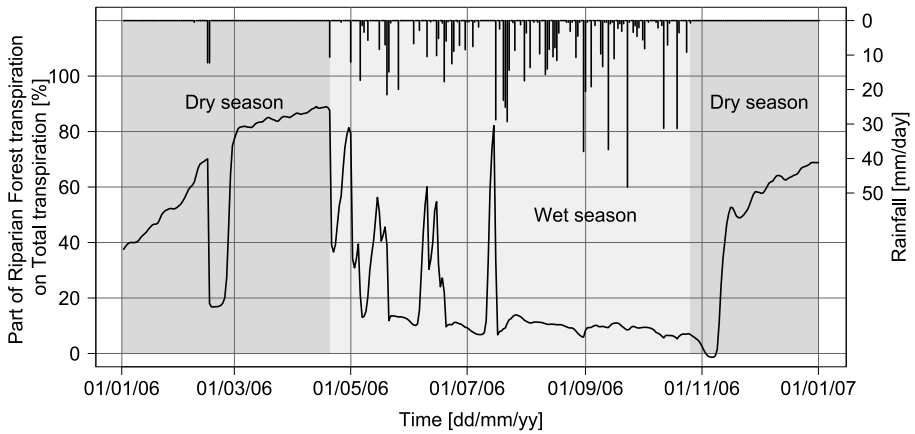

Fig. 10. Part of the riparian forest transpiration on total transpiration (%) for year 2006. This variable is built by subtracting the transpiration of simulation 3 from the transpiration of the base case simulation and then dividing this difference by the transpiration of the base case simulation. Rainfall is plotted on the top, scale being on the right hand side. Shaded areas show the dry season (dark grey) and the wet season (light grey).

HESSD
10, 5643–5686, 2013

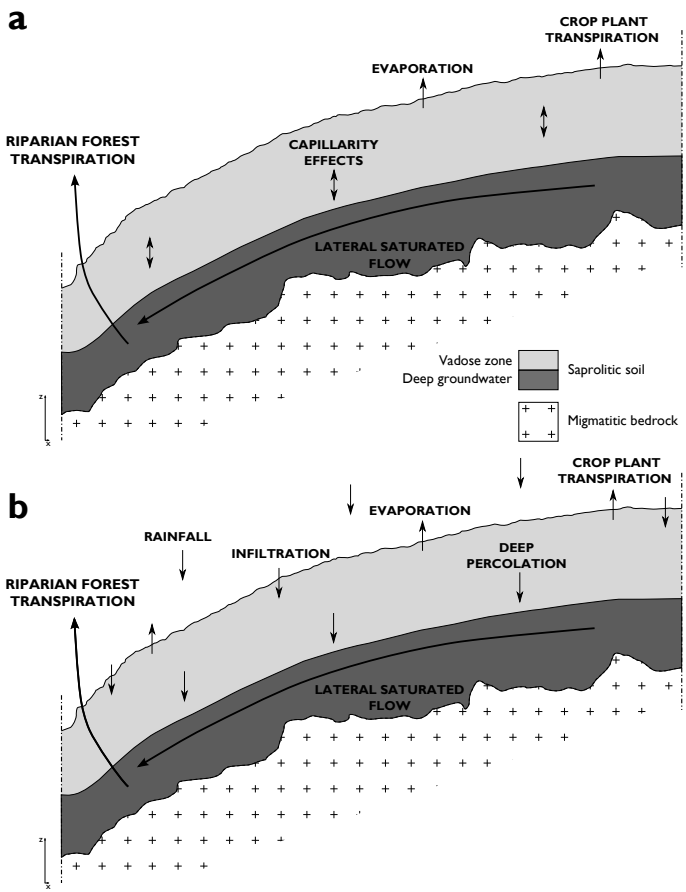

Fig. 11. Schematic hillslope hydrodynamic during the two contrasted seasons: dry season **(a)**, wet season **(b)**. Vertical exaggeration.

HESSD
10, 5643–5686, 2013